Drainage basins and channel incision on Mars

Oded Aharonson*, Maria T. Zuber, Daniel H. Rothman, Norbert Schorghofer, and Kelin X. Whipple

Department of Earth, Atmospheric, and Planetary Sciences, Massachusetts Institute of Technology, Cambridge, MA 02139

Communicated by Sean C. Solomon, Carnegie Institution of Washington, Washington, DC, December 27, 2001 (received for review November 15, 2001)

Measurements acquired by the Mars Orbiter Laser Altimeter on board the Mars Global Surveyor indicate that large drainage systems on Mars have geomorphic characteristics inconsistent with prolonged erosion by surface runoff. We find the topography has not evolved to an expected equilibrium terrain form, even in areas where runoff incision has been previously interpreted. By analogy with terrestrial examples, groundwater sapping may have played an important role in the incision. Longitudinally flat floor segments may provide a direct indication of lithologic layers in the bedrock, altering subsurface hydrology. However, it is unlikely that floor levels are entirely due to inherited structures due to their planar cross-cutting relations. These conclusions are based on previously unavailable observations, including extensive piece-wise linear longitudinal profiles, frequent knickpoints, hanging valleys, and small basin concavity exponents.

Valley networks and channels on Mars were discovered during the Mariner 9 mission (1, 2). Alternatives for their origin have been suggested, but the most widely accepted formation hypothesis is by erosion, and the most likely erosive agent is water (3, 4). The interpretation of ubiquitous erosion by surface runoff has often been taken to imply a warmer, wetter climate on early Mars than the present cold and tenuous atmosphere can support (e.g., refs. 5, and 6). Recent precise observations of Martian topography (7) afford, for the first time, the opportunity to carry out the type of watershed analysis that has been traditionally restricted to Earth, developing quantitative measures relevant to erosion style and intensity.

Channel incision results from both surface runoff and groundwater sapping. The former process results from the shear stresses induced by overland flow, the latter from the removal of material and mass movement as groundwater seeps out to the surface. The relative contributions of surface runoff and groundwater sapping to carving the valley networks and channels on Mars are of primary importance, because large amounts of precipitation required for runoff origin imply climatic conditions that are substantially different from the present ones. If channel incision and drainage basin evolution by runoff erosion are shown to be weak, then requirements for persistent warmer, clement climatic conditions are weakened. However, without rainfall, the problem of recharging the large aquifers necessary for voluminous seepage remains.

Morphometric criteria have been developed to detect incision by groundwater sapping (8–11). A distinction can be made by the change of valley widths, which increases downstream for runoff features but remains essentially constant for sapping features; by the shape of valley heads, which are tapered in rivers but theater-formed for sapping features; and by dendritic networks that are indicative of surface runoff. Such criteria require only planimetric images. Knowledge of the topography permits extension of such analyses by using additional quantitative criteria. Longitudinal stream profiles, locations of channels relative to surface topography, and transverse cross sections of valleys (12, 13) may now be used to constrain the genesis and evolution of Martian valleys.

Method

Watershed analysis of drainage systems carried out here has been developed and tested extensively in terrestrial landscapes (14). The method is used to determine flow direction and local

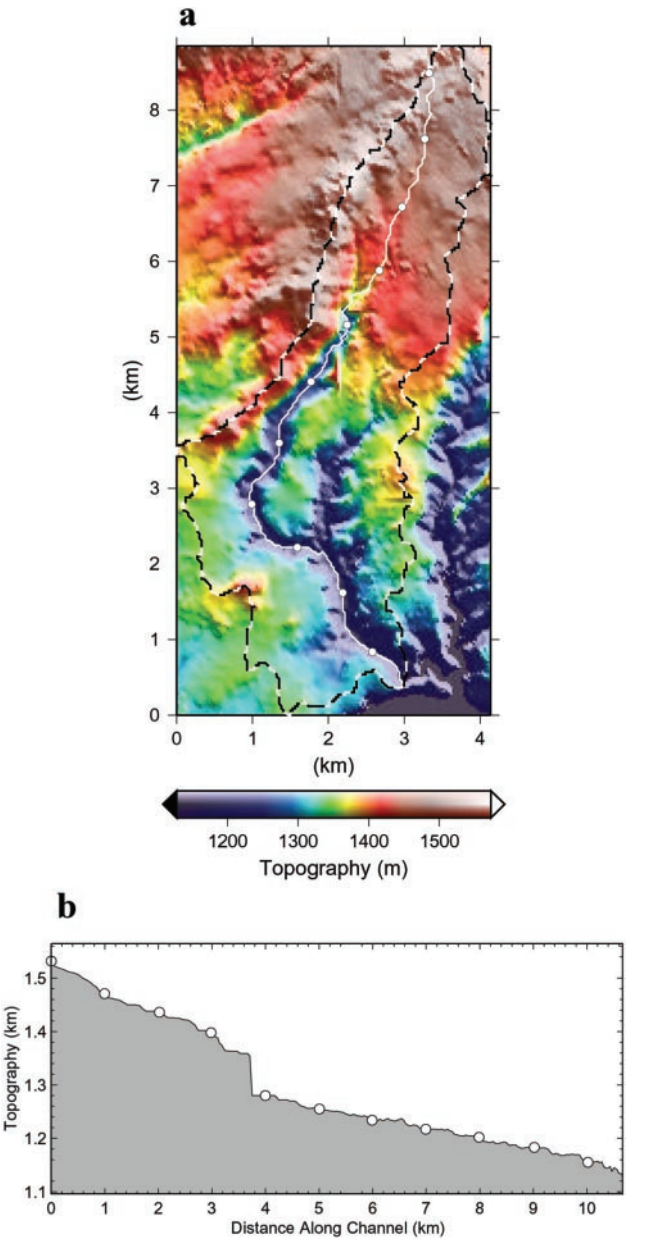

Fig. 1. Topography of Bown's Canyon, Utah. (*a*) Map view and (*b*) longitudinal profile. In *a*, the drainage basin boundary is indicated by a dashed line and the main stream by a solid white line. In both panels, 1-km intervals along the stream are indicated by circles.

*To whom reprint requests should be addressed at: Department of Earth, Atmospheric, and Planetary Sciences, Massachusetts Institute of Technology, Building 54-517, 77 Massachusetts Avenue, Cambridge, MA 02139. E-mail: oded@mit.edu.

The publication costs of this article were defrayed in part by page charge payment. This article must therefore be hereby marked "*advertisement*" in accordance with 18 U.S.C. §1734 solely to indicate this fact.

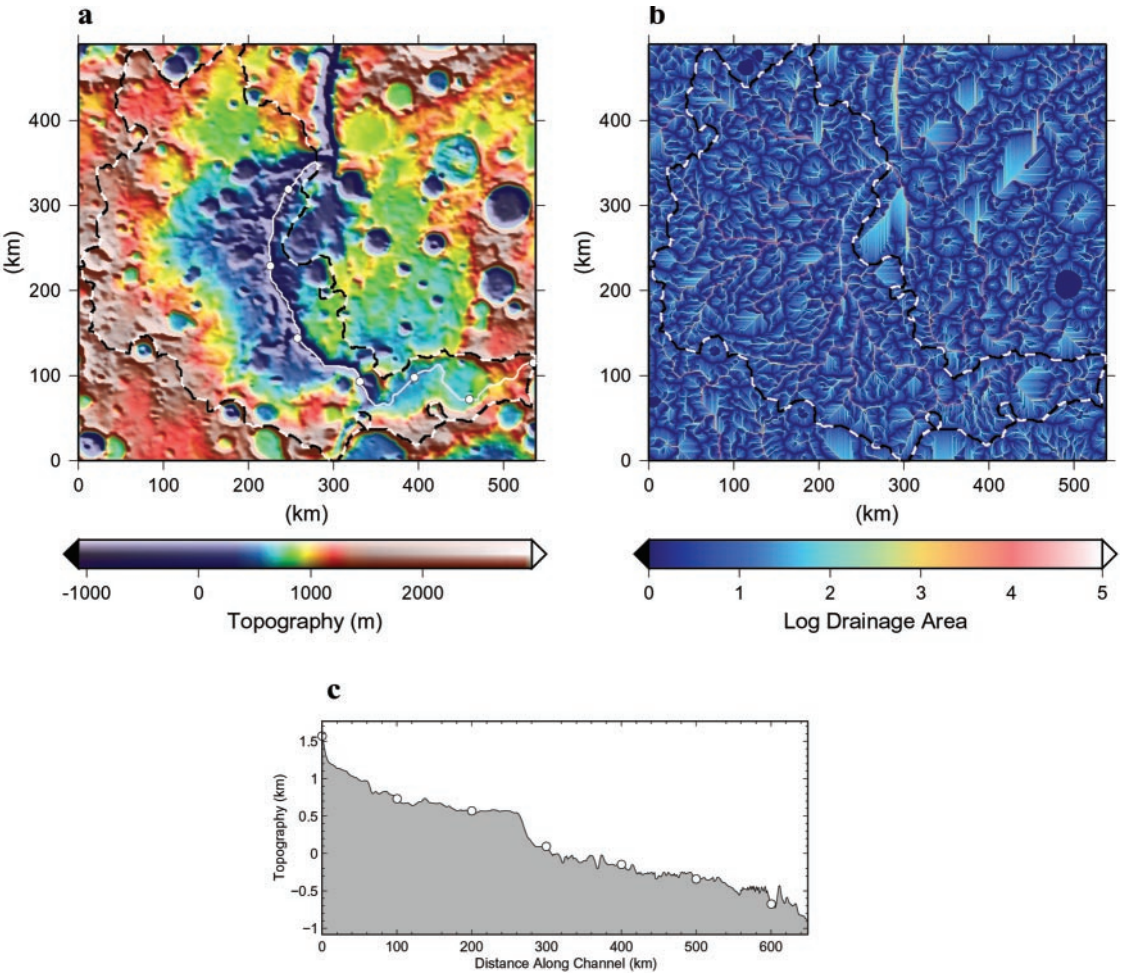

Fig. 2. Topography of Ma'adim Vallis, Mars. (*a*) Map view and (*b*) longitudinal profile. *c* shows a drainage area map, computed by the watershed methodology as described. The basin boundary and main stream are as in Fig. 1. Circles indicate 100-km intervals along the stream. To identify the main channel in the watershed analysis, small pits in the topography have been filled. The longitudinal profile shows unfilled topography.

slope at each grid cell, hence providing the integrated contributing area and the locations of streams and basin boundaries for a given region of interest.

Flow direction for each grid cell is defined by the steepest downhill slope. The slope magnitudes are computed as

$$S(\vec{r}) = \frac{T(\vec{r}) - T(\vec{r}')}{|\vec{r} - \vec{r}'|}, \qquad [1]$$

where $\vec{r}$ and $\vec{r}'$ are the locations of two neighboring cells, and $T(r)$ is the elevation field. For each cell, the eight immediate neighbors are considered. Cells with undefined flow directions are resolved iteratively, by assigning them the direction of their lowest neighbor with a defined flow direction. The total area draining into each cell is referred to as contributing area A. Given a region of interest, the outlet is the cell with the highest drainage area. A main stream is determined by tracing the path of the largest drainage areas, starting from the outlet, until the basin boundary is reached. Smaller "pits" are artificially filled, allowing the computation to proceed through them. The level of the filling is selected such that the flow is uninterrupted in the main channel.

Terrestrial Analog

On Earth, the lower Escalante River, located on the Colorado Plateau, provides a useful analog (8). Although presumably subject to similar climatic conditions, the eastern and western tributary arms of the river have eroded in drastically different styles. Morphological analysis (8) has indicated that tributaries west of the Escalante River evolved primarily by surface runoff erosion. East of the river, channel incision appears to have progressed via head-ward erosion of the cliff face, aided by seepage of groundwater at its base. The topography of runoff channels west of the Escalante River is, almost without exception, concave upwards. Longitudinal profiles along streams are usually smooth. The basins, incised by dendritic networks, exhibit a strong correlation between local slope and contributing area. The main stream typically tends toward the drainage basin center. In contrast, east of the river, the canyon floors are linear or only slightly concave, and individual sections are separated by knickpoints. For example, in Bown's Canyon (Fig. 1), the steep knickpoint in the longitudinal profile (*b*) is clearly seen. The lowest floor segment follows an impermeable lithologic layer identified as the Kayenta Formation, although in places the stream incises through the layer. The overland supply channels for the canyons show no systematic profile shape. Terrain concavity is small or nonexistent, and hence local slope is largely uncorrelated with drainage area. The canyons at this site often tend toward drainage basin boundaries.

Stream Profiles on Mars

Previous models of Martian topography (15) did not permit a reliable quantitative characterization of fluvial morphologies.

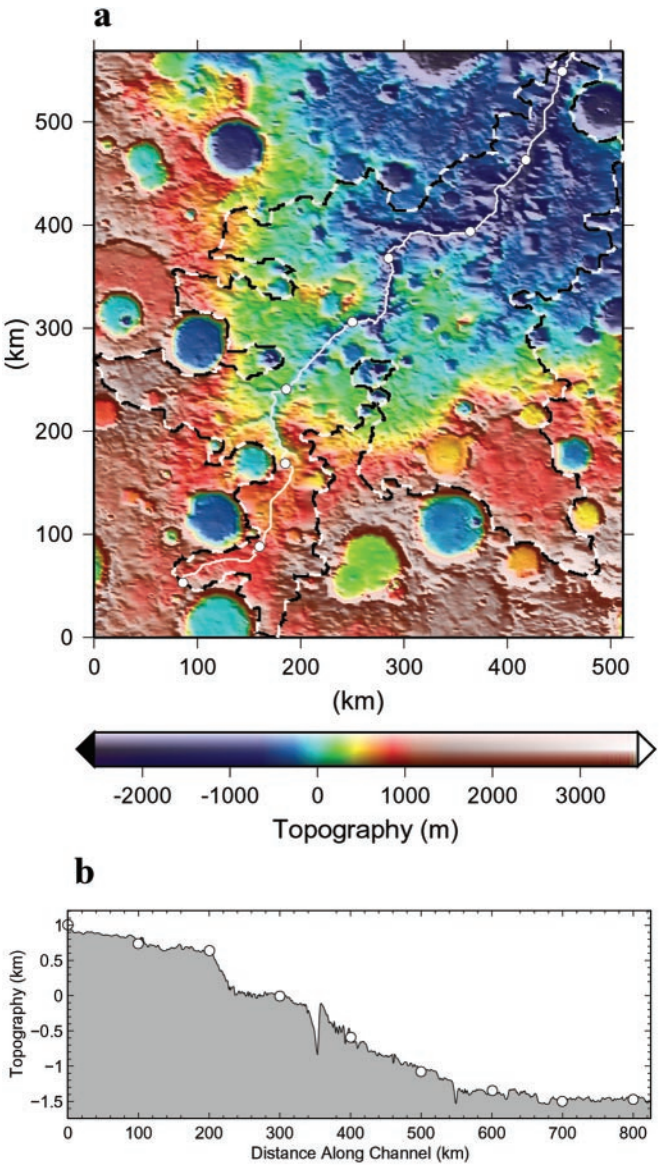

Fig. 3. Topography of Al-Qahira Vallis, Mars. (*a*) Map view and (*b*) longitudinal profile. The basin boundary, main stream, and 100-km intervals are as in Fig. 1.

Photometric and stereo techniques were used to derive local topography (12, 16, 17) but lacked precise slope information. However, recent measurements made by the Mars Orbiter Laser Altimeter (7) on board the Mars Global Surveyor (18) allow construction of a digital elevation model (DEM) from topographic profiles of typical vertical accuracy ~1 m, interpolated on a grid with spatial resolution 1 × 1 km. The derived DEM is undersampled in the latitudinal direction, because along-track shot-spacing is ≈300 m and is oversampled in the longitudinal direction, because track spacing is typically ≈2 km at the equator and decreases poleward.

Several prominent drainage systems on Mars were analyzed. The first example, Ma'adim Vallis, is situated at the north margins of Terra Cimmeria in the southern highlands. The valley is incised in ancient Noachian terrain and drains into Gusev crater in the north. Incision by runoff erosion has been inferred (19–21) on the basis of interpretation of features in Viking images, including V-shaped valleys draining into the main channel trunk and their associated tributary networks. Reclassification as a longitudinal valley was later preferred (4). Sapping processes were later suggested (22) to play a role in carving the valley, with multiple episodes of flow.

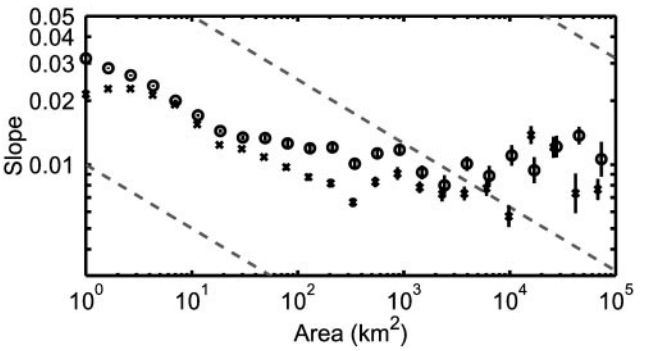

Fig. 4. Slope-area relations for Ma'adim (crosses) and Al-Qahira (circles) Valles. Vertical bars indicate the standard errors in the mean slope. Also shown are reference lines (dashed lines) with concavity exponent $\theta = 0.3$. Because local slope falls off with area more slowly than in known fluvially eroded basins, we deduce that erosion by surface runoff was limited in these areas on Mars.

Drainage basin boundaries and the main stream, as computed by watershed analysis, are shown in a map view of the topography in Fig. 2*a*. The outlet (endpoint) of the stream corresponds to one of the craters superimposed on the channel. Fig. 2*b* shows the longitudinal topography profile of the main stream as a function of distance along the channel. Downstream from approximately 290 km, where drainage area is high, the channel floor has a relatively constant slope (i.e., no concavity is present). A relatively steep knickpoint is present at about 270 km. Uphill, in the first 0–260 km, a small upward concavity is observed. Short convex segments are seen along the profile. Convex segments are particularly prone to erosion and hence attest to the juvenile fluvial character of the system. In addition, in Fig. 2*a*, the bisection of the drainage basin by the main stream is strongly asymmetrical. This geometry is characteristic of terrestrial sapping canyons but is atypical in well developed overland flow (9). Fig. 2*c* shows the contributing area map for this region. To obtain a continuous watershed, a large number of local minima must be artificially filled, reflecting the unevolved nature of the surface with respect to runoff erosion (23). This characteristic is also evident in Fig. 2*c* by the low density of tributaries and the paucity of high-order streams that are not significantly different inside and outside the drainage basin boundaries. Further, drainage density is low when compared with typical terrestrial runoff environments (24, 25).

Although previously considered a runoff channel (e.g., ref. 4 and refs. therein), results from analysis of the Al-Qahira Vallis are similar to those of Ma'adim Vallis in that runoff erosion appears underdeveloped. Fig. 3 shows basin (*a*) and stream (*b*) topography. The stream profile consists of several linear segments, with little or no concavity. Hanging valleys, or tributary streams elevated with respect to the main trunk, are observed at ≈210–360 and ≈360–540 km along channel [also recognized, for example, in Nirgal Vallis (4)]. The deep minimum at ≈350 km along the channel may be a structure that postdates channel formation.

Lithological structures and zones of weakness in Mars' bedrock may be evident in the longitudinally flat floor segments, knickpoints, and hanging valleys. The indication of layers may be independent of the precise nature of the erosion process, as the interface between two layers of different strength or permeability is a likely site of intensified erosion for a range of mechanisms. On smaller scales, pervasive layering has been observed (26, 27) throughout the upper crust, and the groundwater hydrological systems would certainly be controlled by any subsurface structures (4, 28, 29). However, a comparison of strike and dip orientations of planar surfaces fitted to floor profiles reveals that these surfaces are frequently crosscutting even within one valley system. We therefore

conclude that, whereas inherited structures may be responsible for individual stream features, they cannot easily account for the overall topography of the valley system.

Basin Concavity

Many studies in terrestrial drainage environments (e.g., refs. 30–32), laboratory experiments (33), and numerical simulations (34, 35) find general drainage characteristics that are seldom violated. Among these characteristics are smooth valley profiles with distinctive upward-concave shape, equivalent to a local slope decrease in the down-valley direction. This observation is often written in terms of a power law relationship between local slope S and contributing area A,

$$S \sim A^{-\theta}, \quad [2]$$

where θ is the concavity exponent. For terrestrial fluvial systems, the exponent θ is typically in the range 0.3–0.7 (30, 36, 37).

The concavity absent from longitudinal profiles on Mars is also weak in basin averaged quantities. Fig. 4 shows average local slope S plotted against contributing area A for each of the two aforementioned Martian drainage basins. The slope data are sorted in logarithmically spaced bins in A, and the logarithms of the slopes are averaged within each bin. The exponent θ can be inferred from the slope of curves plotted in logarithm–logarithm space. The results for Ma'adim and Al Qahira Valles are consistent: over $\approx$3 orders of magnitude in A, where $A > 30$ km^2, the concavity θ is small. The scatter in the slopes introduces variability in θ, and S only weakly depends on A. Also shown for reference are lines corresponding to $\theta = 0.3$, a value that is comparatively low but still appropriate for some terrestrial runoff environments (37, 38). In the range of high drainage areas, fits to the averaged slope data yield values for θ indistinguishable from those expected for random topography (39). Hence, slope-area relations show no evidence for extensive fluvial sculpting of the terrain in an environment where flow discharge increases steadily downstream, as would be expected for sustained runoff-driven erosion. At the low drainage area supply region, where $A < 30$ km^2, θ is in the range 0.2–0.3, consistent with expectations for transport-limited erosion of fine-grained material (38). However, even the slightly higher exponent at lower drainage areas is similar to that observed for undissected topography of Mars and Earth, as well as some random surfaces (39).

Summary

Similar results are obtained for other fluvial systems on Mars, such as Nanedi Vallis and canyons on the south wall of Valles Marineris (9). Although several processes and a complex evolutionary history may be required to explain fluvial features on Mars, we find that, for the examples considered here, surface runoff appears to have played at most a superficial role in the evolution of the Martian landscape. The relative infrequency of dissection over much of the Martian surface (24, 25), down to the scales of highest-resolution images (40), has also been used to argue against voluminous runoff and the required implication of an early warm climate. Morphologic evidence for surface runoff certainly exists (6), but the results here indicate that there has not been a significant amount of landscape evolution by fluvial erosion in areas where runoff incision has been previously interpreted. Although other valley incision processes are not ruled out by this analysis, multiple physiographic characteristics support groundwater sapping as an important contributor to the formation of the channels examined.

Taken together, these topographically derived measurements indicate that the channels and associated drainage basins considered here have not been subject to significant sustained runoff erosion. Dendritic networks have long been observed near Ma'adim and Al-Qahira Valles, and their topographic properties appear in low-drainage area regions. The emerging picture is that the large volumes of incision are relatively unevolved with respect to overland runoff erosion, and runoff networks incise the surface superficially at uphill source regions. Although the topography of an individual segment may be lithologically controlled, extensive layers are inconsistent with the orientations of multiple segments within the drainage systems. Quantitative analysis of fluvial topography, in concert with further study of terrestrial analogs, holds the promise of evaluating the extent to which lithologic heterogeneity, intensity of erosion, and erosion process have influenced the morphology of river channels and hence the ancient hydrology of Mars.

We acknowledge helpful reviews from Mike Carr and Vic Baker, and discussions with Roger Phillips, Rebecca Williams, Robert Craddock, and Noah Snyder. This study was supported by the generous Kerr Fellowship, the Mars Global Surveyor Project, and by Department of Energy Grant DE FG02-99ER 15004.

1. McCauley, J. F., Carr, M. H., Cutts, J. A., Hartmann, W. K., Masursky, H., Milton, D. J., Sharp, R. P. & Wilhelms, D. E. (1972) *Icarus* **17,** 289–327.
2. Masursky, H. (1973) *J. Geophys. Res.* **78,** 4009–4030.
3. Carr, M. H. (1981) *The Surface of Mars* (Yale Univ. Press, New Haven, CT).
4. Baker, V. R. (1982) *The Channels of Mars* (Univ. of Texas Press, Austin, TX).
5. Sagan, C., Toon, O. B. & Gierasch, P. J. (1973) *Science* **181,** 1045–1049.
6. Craddock, R. A. & Howard, A. D. *J. Geophys. Res.*, in press.
7. Smith, D. E., Zuber, M. T., Frey, H. V., Garvin, J. B., Head, J. W., Muhleman, D. O., Pettengill, G. H., Phillips, R. J., Solomon, S. C., Zwally, H. J., *et al.* (2001) *J. Geophys. Res.* **106,** 23689–23722.
8. Laity, J. E. & Malin, M. C. (1985) *Geol. Soc. Am. Bull.* **96,** 203–217.
9. Kochel, R. C. & Piper, J. F. (1986) *J. Geophys. Res.* **91,** E175–E192.
10. Gulick, V. C. & Baker, V. R. (1990) *J. Geophys. Res.* **95,** 14325–14344.
11. Gulick, V. C. (2001) *Geomorphology* **37,** 241–268.
12. Goldspiel, J. M. & Squyres, S. W. (2000) *Icarus* **148,** 176–192.
13. Williams, R. M. E. & Phillips, R. J. (2001) *J. Geophys. Res.* **106,** 23737–23751.
14. Tarboton, D. G. (1997) *Water Resource Res.* **33,** 309–319.
15. Esposito, P. B., Banerdt, W. B., Lindal, G. F., Sjogren, W. L., Slade, M. A., Bills, B. G., Smith, D. E. & Balmino, G. (1992) in *Mars*, eds. Kieffer, H. H., Jakosky, B. M., Snyder, C. W. & Matthews, M. S. (Univ. of Arizona Press, Tucson, AZ), pp. 209–248.
16. Pieri, D. C. (1980) *Science* **210,** 895–897.
17. Goldspiel, J. M., Squyres, S. W. & Jankowski, D. G. (1993) *Icarus* **105,** 479–500.
18. Albee, A. L., Arvidson, R. E., Palluconi, F. & Thorpe, T. (2001) *J. Geophys. Res.* **106,** 23291–23316.
19. Sharp, R. P. & Malin, M. C. (1975) *Geol. Soc. Am. Bull.* **86,** 593–609.
20. Masursky, H., Boyce, J. V., Dial, A. L., Schabert, G. G. & Strobell, M. E. (1977) *J. Geophys. Res.* **82,** 4016–4037.
21. Carr, M. H. & Clow, G. D. (1981) *Icarus* **48,** 91–117.
22. Cabrol, N. A., Grin, E. A. & Landheim, R. (1998) *Icarus* **132,** 362–377.
23. Banerdt, W. B. & Vidal, A. (2001) *Lunar Planet. Sci.* **XXXII,** no. 1488.
24. Carr, M. H. (1995) *J. Geophys. Res.* **100,** 7479–7507.
25. Carr, M. H. & Chuang, F. C. (1997) *J. Geophys. Res.* **102,** 9145–9152.
26. Malin, M. C., Carr, M. H., Danielson, G. E., Davies, M. E., Hartmann, W. K., Ingersoll, A. P., James, P. B., Masursky, H., McEwen, A. S., Soderblom, L. A., *et al.* (1998) *Science* **279,** 1681–1685.
27. Malin, M. C. & Edgett, K. S. (2000) *Science* **290,** 1927–1937.
28. Baker, V. R., Strom, R. G., Gulick, V. C., Kargel, J. S., Komatsu, G. & Kale, V. S. (1991) *Nature (London)* **352,** 589–594.
29. Clifford, S. M. (1993) *J. Geophys. Res.* **98,** 10973–11016.
30. Flint, J. J. (1974) *Wat. Resource Res.* **10,** 969–973.
31. Howard, A. D. & Kerby, C. (1983) *Geol. Soc. Am. Bull.* **94,** 739–752.
32. Whipple, K. X., Kirby, E. & Brocklehurst, S. H. (1999) *Nature (London)* **401,** 39–43.
33. Howard, A. D. & McLane, C. F. (1988) *Water Resource Res.* **24,** 1659–1674.
34. Willgoose, G., Bras, R. L. & Rodriguez-Iturbe, I. (1991) *Water Resource Res.* **27,** 1697–1702.
35. Howard, A. D. (1994) *Water Resource Res.* **30,** 2261–2285.
36. Tarboton, D. G., Bras, R. L. & Rodriguez-Iturbe, I. (1989) *Water Resource Res.* **25,** 2037–2051.
37. Whipple, K. X. & Tucker, G. E. (1999) *J. Geophys. Res.* **104,** 17661–17674.
38. Howard, A. D., Dietrich, W. E. & Seidl, M. A. (1994) *J. Geophys. Res.* **99,** 13971–13986.
39. Schorghofer, N. & Rothman, D. H. (2001) *Phys. Rev. E* **63,** 026112, 1–7.
40. Malin, M. C. & Carr, M. H. (1999) *Nature (London)* **397,** 589–591.